21.2 A CMOS Single-Chip Electronic Compass with Microcontroller

Christian Schott[1], Robert Racz[1], Samuel Huber[1], Angelo Manco[1], Markus Gloor[1], Nicolas Simonne[2]

[1]Melexis, Bevaix, Switzerland
[2]Melexis, Tessenderlo, Switzerland

We present a CMOS single-chip electronic compass that includes all the digital signal processing required for an accurate heading calculation. The sensor is realized in a 0.35µm low-voltage CMOS technology with integrated magnetic concentrator (IMC) post-process [1,2]. The IMC process has recently been fully automotive qualified for another product [3], where it is now used in volume production.

The device's analog part consists of a 3-axis magnetic field transducer based on Hall elements, and amplifiers. A 12b ADC converts the amplified signals into the digital domain where a 16b microcontroller calculates the heading information and outputs it via a serial interface. The block diagram in Fig. 21.2.1 shows the architecture and signal flow of the circuit.

The 3-axis magnetic field transducer is based on a total of 12 Hall elements (4 for each axis) in combination with a structured IMC metal layer, which is directly bonded to the CMOS wafer (Fig. 21.2.2). This 3-axis field transducer generates 3 Hall voltages V_x, V_y and V_z, corresponding to the 3 magnetic field components B_x, B_y and B_z. The IMC structure realizes a passive gain of about 8 for the horizontal components, B_x and B_y. The Hall elements are realized in a pinched n-well with a cross-shaped geometry, and have an active area of about 15×15µm^2.

IMC technology generally allows the measurement of any in-plane magnetic field component (Fig. 21.2.3). It is based on the principle that flux lines parallel to the chip surface are deflected locally under the edge of the ferromagnetic flux concentrator so that they can be measured by conventional CMOS Hall elements. This principle is particularly adapted to realize accurate angle sensors [2].

The IMC structure of the electronic compass is implemented in the shape of five octagonal rings, instead of the circular rings used in [4]. This structure is used because the etching of a constant-width airgap between octagons is easier to control than the etching of a concave gap between rings, leading to a more robust device with smaller mismatch between the sensitivities in the two axes. The sensor additionally contains a circuit block for "low-energy" demagnetization of the ferromagnetic concentrator, to eliminate remnant magnetization caused by strong accidentally-applied external fields. The degaussing coil is a single-turn loop through the IMC ring structures, whose lower part is implemented as integrated metal tracks and whose upper part is finished during packaging by bonding connection.

As shown in Fig. 21.2.4, the Hall elements are current biased and the spinning current technique is used to modulate the Hall voltages to 25kHz. This prevents the offset voltages of the Hall elements from saturating the amplifiers. The fully differential amplification chain consists of three stages, and has a programmable analog gain, which can be varied between 312.5 and 20000. The stages are connected via high-pass filters for further elimination of any DC offset voltages. After demodulation, the signal is passed through an 8kHz LPF.

The ADC uses an extended counting technique [5], which is a blend of ΔΣ modulation, with its high resolution but relatively low speed, and algorithmic conversion with its higher speed but lower accuracy. The converter is operated first as a first-order ΔΣ modulator (counting phase) to convert the MSB's, and then the same hardware is used as an algorithmic converter (extended phase) to convert the remaining LSB's. The ADC operates at low current (typ. 250µA) and low sampling frequency (400kHz) and is programmable between 15 and 18 bits, of which only the 12 MSBs are used. Between 512 and 4096 samples are integrated during the counting phase.

The digitized data are transmitted to an on-chip microcontroller, where they are first passed through a 100Hz digital LPF for further noise reduction. Then the angle of the applied magnetic field (earth's field) is computed with the help of a firmware algorithm stored in the ROM. This heading information is then output to an external host microcontroller via the digital interface. By using the on-board EEPROM, parameters like offset fields, axis selection, analog gain, zero setting and interface protocol (I2C or SPI) can be defined. These parameters allow the end-user to entirely calibrate the single-chip compass even in the presence of magnetic field distortions caused by ferromagnetic objects (e.g., batteries, sensor housing, car body). Four analog inputs from external sensors can also be digitized. The results are transmitted to a host system via an on-board digital interface.

The sensor chip has been realized in a low-voltage 0.35µm mixed-signal CMOS technology (Fig. 21.2.5). After completion of the CMOS process, the IMC layer is applied and photolithographically defined. The on-chip degaussing coil is then completed during the wire bonding to the package leadframe. The compact die size of 2.3×2.8mm^2 allows for packaging into a standard 20-pin plastic package, which measures only 5mm×4mm×1mm. Due to rigorous low-voltage design of all circuit parts, the compass sensor works within a supply range of 2.2 to 3.6V and features a current consumption of 5mA in normal power mode and less than 2mA in low-power mode.

The X- and Y-axis sensitivities are programmable between 0.9 and 58 LSB/µT, while the Z-axis sensitivity is about 8 times smaller due to the lack of IMC gain. The sensor's nonlinearity was measured by a magnetic field sweep from 500 to -500µT, and was found to be below 5µT. The onset of magnetic saturation of the IMC is observed to be above 1mT. The sensor offset along the X and Y axes corresponds to a value within ±10µT, which can be digitally compensated. Offset drift over the temperature range from -25 to +100°C at a sensitivity of 7.25LSB/µT is about 100LSB (Fig. 21.2.6). This drift is relatively high compared to other recent work [6] and it has its origin in the variation of local stress with temperature under the edge of the IMC where the Hall elements are placed. However, it is reduced to <10 LSB after calibration, which corresponds to about 1µT.

The output characteristics of the packaged sensor were measured by using a 3D Helmholtz coil. The angular error of 1.5° maximum was measured by rotating the sensor within the earth's magnetic field at constant temperature (Fig. 21.2.7). The heading resolution is better than 0.5° and the accuracy better than ±2°.

Possible host systems for such a miniature complete electronic compass system range from watches to mobile phones to automobiles. Due to its 3-axis operation, the compass can either be used as conventional heading sensor, or as a recalibration reference for gyroscopes in more complex systems, or even as a 3-axis low-field transducer in mapping applications.

References:

[1] Patent application EP772046W
[2] R. S. Popovic, R. Racz and C. Schott, "A New CMOS Hall Angular Position Sensor," *tm – Technisches Messen,* 68, June 2001, pp. 286-291.
[3] Melexis product MLX90316 - see http://www.melexis.com
[4] Robert Racz, C. Schott and Samuel Huber, "Electronic Compass Sensor," *Proc. IEEE Sensors*, vol. 3, pp. 1446- 1449, Oct., 2004.
[5] P. Rombouts and L Weyten, "A versatile Nyquist-rate A/D Converter with 16-18 bit Performance for Sensor Readout Applications," *Elsevier Integration, VLSI J.*, vol. 39, no. 1, pp. 48-61, 2005.
[6] J. van der Meer et al., "A Fully-Integrated CMOS Hall Sensor with a 3.65µT 3σ Offset Spread for Compass Applications," *ISSCC Dig. Tech. Papers*, pp. 246-247, 2005.

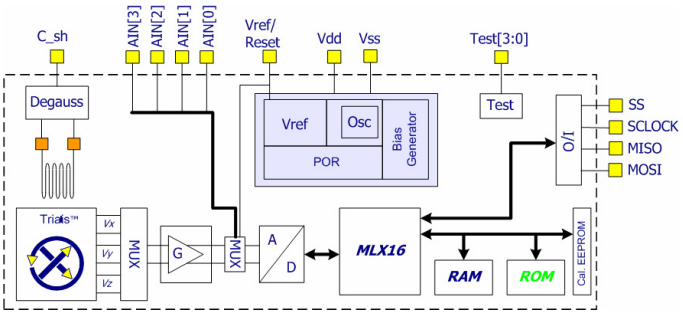

Figure 21.2.1: Block diagram of the electronic compass.

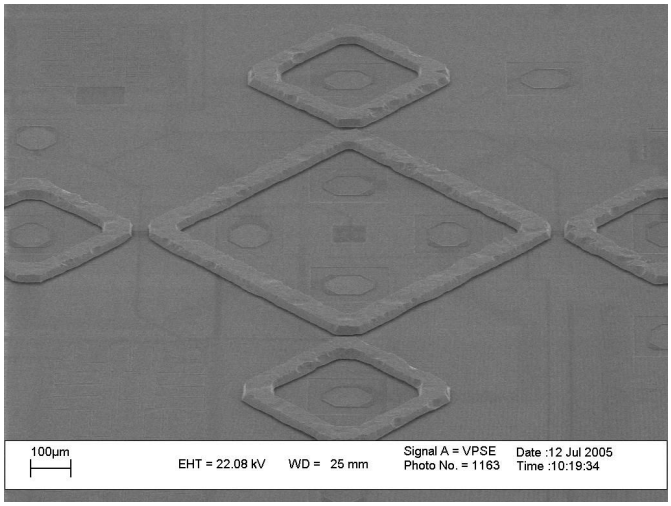

Figure 21.2.2: SEM photograph of the magnetic concentrator.

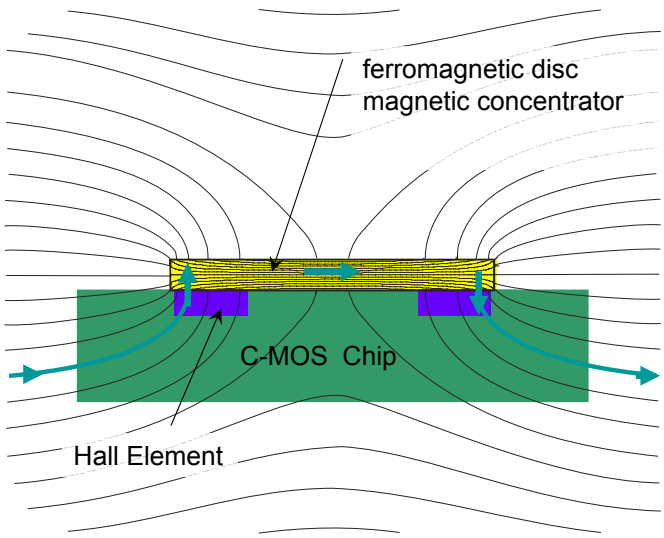

Figure 21.2.3: Working principle of the IMC (local field rotation and amplification).

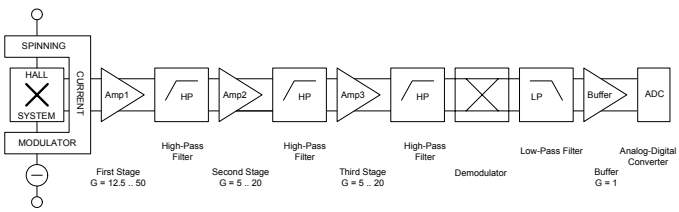

Figure 21.2.4: Hall Front-end and analog amplification chain.

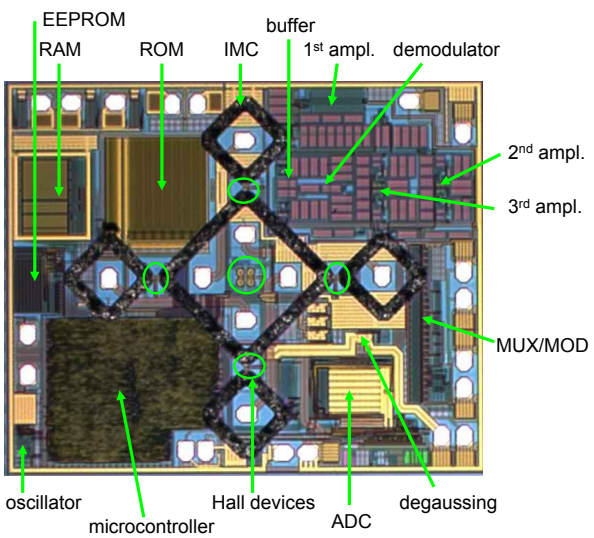

Figure 21.2.5: Micrograph of silicon die with IMC.

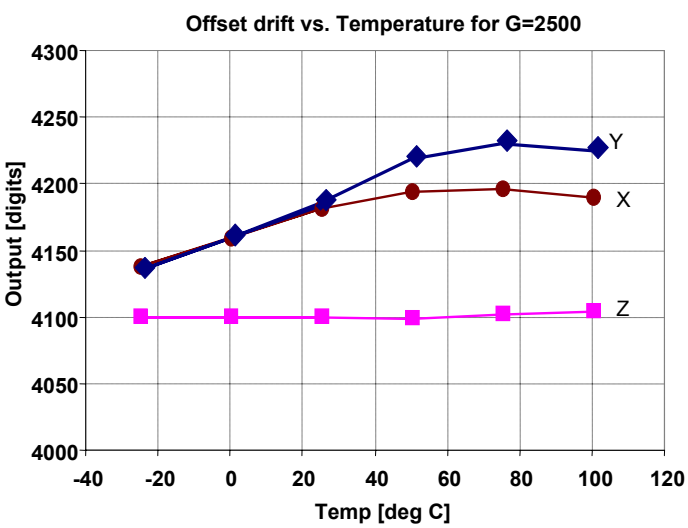

Figure 21.2.6: Offset-drift versus temperature (7.25LSB/µT).

Continued on Page 609

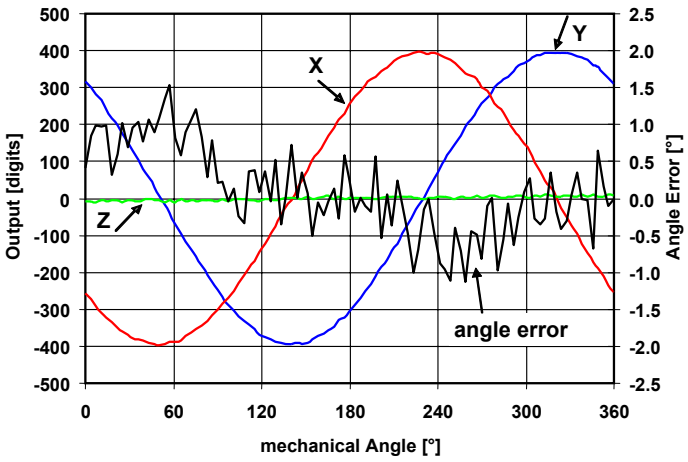

Figure 21.2.7: Output angle error over 360° rotation in the earth's magnetic field.

